

# New Connection Design of High Power Bolted Busbar Connections

RAINA TZENEVA<sup>1</sup>, YANKO SLAVTCHEV<sup>2</sup> and VALERI MLADENOV<sup>3</sup>

<sup>1</sup>Department of Electrical Apparatus, Faculty of Electrical Engineering, Technical University of Sofia  
8, Kliment Ohridski St, Sofia-1000, BULGARIA

<sup>2</sup>Department of Logistics and Materials Handling, Technical University of Sofia  
8, Kliment Ohridski St, Sofia-1000, BULGARIA

<sup>3</sup>Department of Theoretical Electrical Engineering, Faculty of Automatics, Technical University of Sofia  
8, Kliment Ohridski St, Sofia-1000, BULGARIA

**Abstract:** - The paper reported discusses how introducing a slotted hole shape or groups of small holes around the bolt holes in high power bolted busbar connections increases significantly the true contact area and therefore reduces contact resistance. The new designs, formally called S, SH and G type are compared with the classical one of bolted busbar connections by the help of several computer models. It has been estimated that the new cases lead to a considerable raise in contact pressure  $P$  and contact penetration  $\mu$  in the contact interface between the busbars.

**Key-Words:** - Bolted busbar high power connections, Contact pressure, Contact penetration, Contact resistance, New connection design

## 1. Introduction

Steadily increasing energy consumption in densely populated regions imposes severe operation conditions on transmission and distribution systems which have to carry greater loads than in the past and operate at higher temperatures.

Power connections are generally the weak links in electrical transmission and distribution systems – both overhead and underground systems.

Mainly, there are two factors that affect the reliability of a power connection. The first is the design of the connection and the material from which it is fabricated. The second is the environment to which the connection is exposed.

The fundamental requirements for the design of reliable high-power connections used in bare overhead lines are given in [1]. The fundamental design criteria for power connectors are: maximization of electric contact true area, optimization of frictional forces with conductors (buses), minimization of creep and stress relaxation, minimization of fretting and galvanic corrosion, minimization of differential thermal expansion along and normal to interfaces. Summarizing the major connection design criteria, mentioned above it is worthwhile noting that all the criteria can be met simultaneously by working out an outline that achieves a sufficiently large contact load, a large area of metal-to-metal contact and sufficient elastic energy storage in the connection to maintain an acceptable connector's contact load throughout the service life of the connection.

## 2. Theoretical background

All joint surfaces are rough and their surface topography shows summits and valleys. Thus under the joint force  $F$  two joint surfaces get into mechanical contact only at their surface summits. Electrical current lines are highly constricted at the contact spots when passing through, as presented schematically in Fig. 1a. This constriction amplifies the electric flow resistance and hence the power loss. Obviously, the more the contact spots, the smaller the power loss at the interface of the conductors. Power connections with superior performance are designed to maximize both the number and the life of the contact spots.

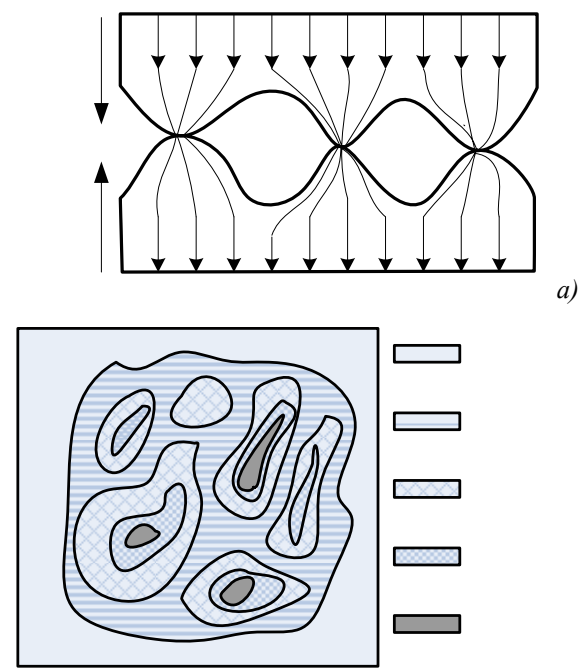


Fig.1: a) Contact surface and current lines; b) Contact area with  $a$  spots

For this reason, it is essential to keep in mind that the load bearing area in an electric joint is only a fraction of the overlapping, known as apparent area. Metal surfaces, e. g. those of copper conductors are often covered with oxide or other insulating layers. As a consequence, the load bearing area may have regions that do not contribute to the current flow since only a fraction of may have metallic or quasi-metallic contact and the real area of electric contact, i.e. the conducting area, could be smaller than the load bearing area (Fig. 1b) [2].

A conducting area is referred to as quasi-metallic when it is covered with a thin ( $< 20\text{\AA}$ ) film that can be tunneled through by electrons. This quasi-metallic electric contact results in a relatively small film resistance  $R_f$ .

The summits of the two electric joint surfaces, being in metallic or quasi-metallic contact, form the so called  $\alpha$ -spots where the current lines bundle together causing the constriction resistance  $R_c$ . The number  $n$ , the shape and the area of the  $\alpha$ -spots are generally stochastic and depend on material parameters of the conductor material, the topography of the joint surfaces and the joint force. For simplicity it is often assumed that the  $\alpha$ -spots are circular. Looking at one single circular  $\alpha$ -spot its constriction resistance  $R_c$  depends on its radius  $a$  and the resistivity  $\rho$  of the conductor material. Under the assumption that the bulk material above and under the  $\alpha$ -spot is infinite in volume, the value of the constriction resistance can be calculated by means of the Holm's ellipsoid model.

$$R_c = \frac{\rho}{2a} \tag{1}$$

If a single  $\alpha$ -spot is completely covered with a thin film of resistivity  $\rho_f$  and thickness  $s$ , its film resistance  $R_f$  is given by

$$R_f = \frac{\rho_f s}{\pi a^2} = \frac{\sigma_f}{\pi a^2} \tag{2}$$

where  $\sigma_f$  is the tunnel resistivity i.e. the resistance of the film across one  $\text{cm}^2$ .

The total resistance  $R_1$  of a  $\alpha$ -spot, referred to as contact resistance, results in the sum of the constriction resistance  $R_c$  and the film resistance  $R_f$

$$R_1 = R_c + R_f \tag{3}$$

### 3. Modeling bolted busbar connection

In this paper an attempt to compare 3 new designs of high power bolted busbar connections (slotted bolt holes - design S, slotted bolt holes, ending with small holes - design SH and groups of small holes around the bolt holes - design G is made. The mechanical changes,

associated with the contact penetration depth and the contact pressure, in the contact area between two busbars in a bolted busbar connection are studied by the help of the finite elements simulation tool ANSYS Workbench. If a higher contact penetration increases  $\alpha$ -spots both in numbers and dimensions, which in turn expands the true contact area and decreases contact resistance, then a new hole-shape could be introduced for this connection. A typical bolted busbar connection is shown in Fig. 2.

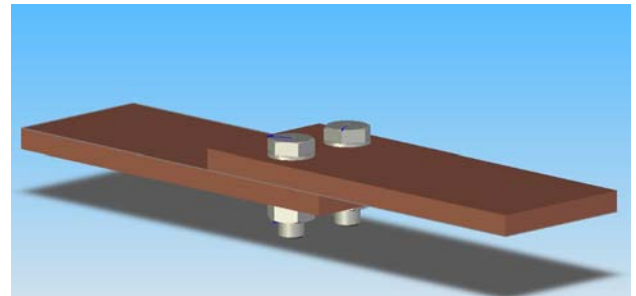


Fig. 2: Bolted busbar connection

The new slotted hole shape arises from [3]. Boychenko and Dzektsler have shown that changing the connection design can equally be effective in increasing the contact area. In other words, cutting slots in the busbar in a manner as shown in Fig. 3, the actual surface area of a joint can be increased by 1.5 to 1.7 times of that without slots. The contact resistance of joint configuration with slots (b) is 30-40% lower than that of (a) and is mechanically and electrically more stable when subjected to current cycling test [4], [5]. The beneficial effect of sectioning the busbar is attributed to a uniform contact pressure distribution under the bolt, which in turn, creates a larger contact area. This case is investigated in [6].

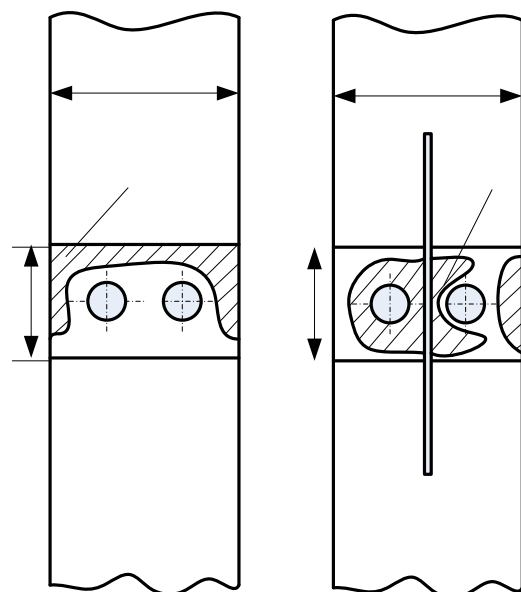


Fig. 3: Effect of making a slot in the overlapping busbar joint

This idea is developed in [7], [8] and a new slotted hole shape for bolted high power connections – **design S** is proposed. Fig. 4 shows the hole shape of the 11 investigated cases. A significant rise in  $P$  and  $\mu$  is obtained.

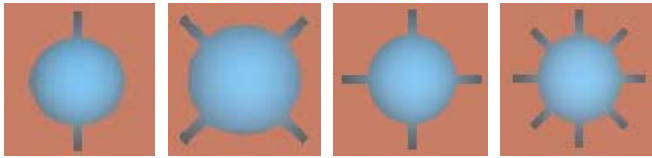


Fig. 4: Hole shape with 2, 4 or 8 slots

The cases are as follows:

case1– classical case – copper busbars with 2 bolt holes;

case2– the slots are parallel to the busbar axis;

case3– the slots are perpendicular to the busbar axis;

case4– mixed case – one of the busbars belongs to case 2 and the other one to case 3;

For cases 2 to 4 all bolt holes have two slots of length 3mm and width 1mm.

In cases 5 to 8 the busbar holes have 4 slots, 3mm long with variable width, arranged in such a way that the pairs of slots are on mutually perpendicular axes, rotated at 45 degrees about the busbar axes. Widths are:

case 5 – 0.3mm; case 6 – 0.5mm;

case 7 – 0.7mm; case 8 – 1mm;

case 9 – the 4 slots are not rotated;

case 10 – mixed – the first busbar corresponds to case 8 and the second one to case 9;

case 11 – a busbar hole with 8 slots of length 3mm and width 1mm;

All the cases are supposed to: decrease radial loadings on bolts that emerge after the connection is assembled; increase the  $\mu$  in the busbars near the bolts area; maximize the true area of metal to metal contact in an electrical interface.

The investigated assembly consists of:

□ Copper busbars (Young’s modulus  $E = 1.1 \cdot 10^{11} \text{Pa}$ , Poisson’s ratio  $\mu = 0.34$ , width 60mm, height 10mm, length 160mm, busbars’ overlap 60mm with 2 holes of  $\text{Ø}10.5\text{mm}$ ;

□ Fasteners: bolts – Hex Bolt GradeB\_ISO 4015 – M10 x 40 x 40 – N, steel  $E = 2.10^{11} \text{Pa}$ ,  $\mu = 0.3$ ; nuts – Hex Nut Style1 GradeAB\_ISO 4032 – M10 – W – N, steel  $E = 2.10^{11} \text{Pa}$ ,  $\mu = 0.3$ ; washers – Plain Washer Small Grade A\_ISO 7092 – 10, steel  $E = 2.10^{11} \text{Pa}$ ,  $\mu = 0.3$ . Tension in each bolt  $F = 15000\text{N}$ .

Models are studied for contact pressure  $P[\text{MPa}]$  and penetration  $\mu[\mu\text{m}]$  within the busbars electrical interface.

The  $\mu$  for case 8 is shown in Fig.5. When the 4 slots are introduced the high penetration zone expands covering the region between the slots.

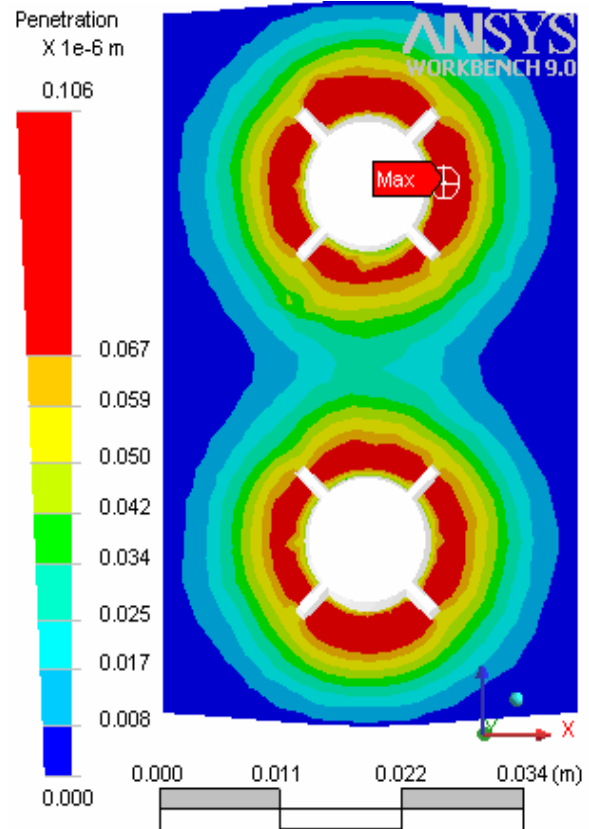


Fig.5: Contact penetration for case 8 with 4 slots

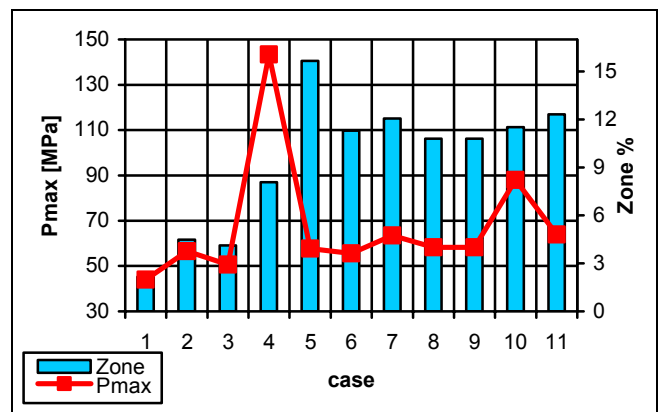


Fig.6: Max contact pressure and % occupation of the zone of  $P > 38.86 \text{MPa}$  for all cases - design S

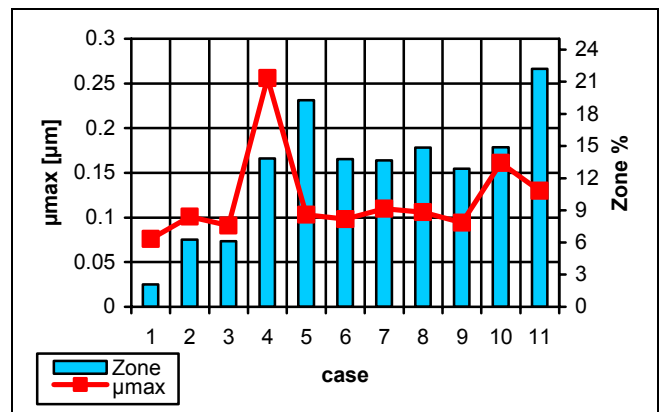


Fig.7: Max contact penetration and % occupation of the zone of  $\mu > 0.0673 \mu\text{m}$  for all cases – design S

All the eleven cases have been evaluated by comparing the max P and  $\mu$  values for each one of them as well as the % participation of the 8 zones according to the legends. With that end in view, all zones are set to equal upper and lower limits. Thus the comparison procedure is performed by the help of the Adobe Photoshop software, where each colored zone is identified with a certain number of pixels. Fig 6 and Fig.7 summarize the results.

Considered next is **design SH**, investigated in details in [9] and illustrated in Fig. 8. The new shape is that of bolt hole slots ending with small circular gaps. There is ample of P and  $\mu$  data gathered.



Fig. 8: Bolt hole slots, ending with small circular gaps

Table I describes the 11 investigated cases of different slot width and radius of the small circular holes.

Table 1

Case No	1	2	3	4	5	6	7	8	9	10	11
Slot width, mm	0	0.3	0.3	0.3	0.3	0.5	0.5	0.5	0.7	0.7	1.0
Small hole radius, mm	0	0.3	0.5	0.7	1.0	0.5	0.7	1.0	0.7	1.0	1.0

The model, given in Fig.9, proves that the SH design leads to high P and  $\mu$  values around the slots.

The charts in Fig.10 and Fig.11 summarize the results and compare the values with the classical case.

Cutting thin slots in copper or aluminum poses certain difficulties that could be overcome effectively by changing the slots with groups of two or four small holes - **design G**.

There have been studied 13 different design G cases.

case 1– classical case – copper busbars with 2 bolt holes;

case 2– two horizontal groups of two holes of diameter  $\varnothing 1$ mm and distance of 0.9mm between the holes, parallel to the busbar axis;

case 3– two vertical groups of two holes of diameter  $\varnothing 1$ mm and distance of 0.9mm between the holes;

case 4– mixed case – one of the busbars in the connection is of case 2 and the other one is of case 3;

case 5 – eight groups of two holes of diameter  $\varnothing 1$ mm and distance of 0.9mm between the holes, displaced at angle of 45 degrees;

case 6 – two horizontal groups of three holes of diameter  $\varnothing 0.8$ mm and distance of 0.2mm between the holes, parallel to the busbar axis;

case 7 – two vertical groups of three holes of diameter  $\varnothing 0.8$ mm and distance of 0.2mm between the holes;

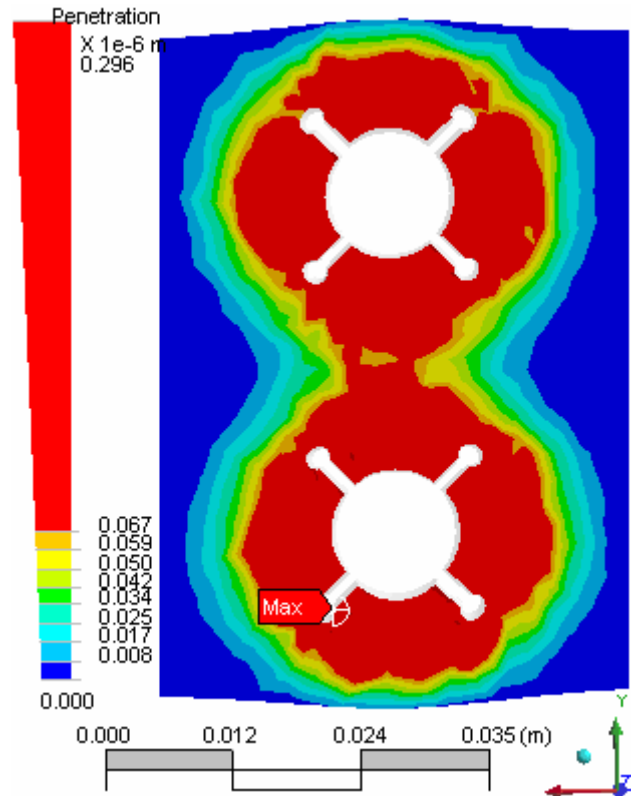


Fig. 9: Contact penetration for case 11

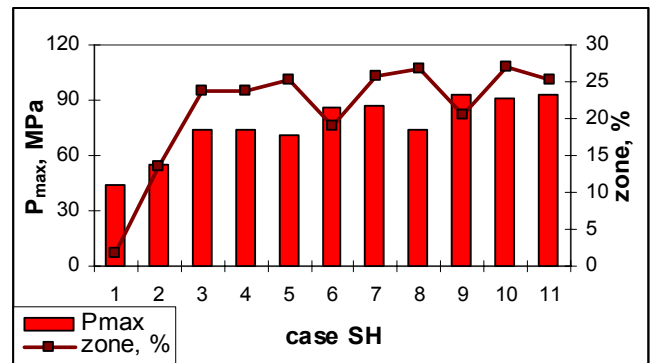


Fig.10: Max contact pressure and % occupation of the zone of P > 38.86MPa for all cases – design SH

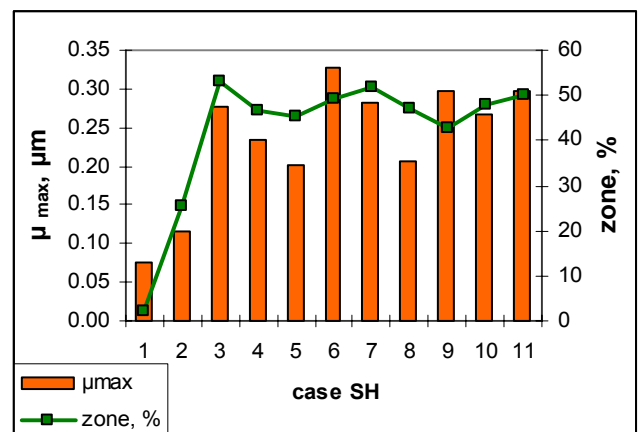


Fig.11: Max contact penetration and % occupation of the zone of μ > 0.0673μm for all cases – design SH

case 8 –four groups (two horizontal and two vertical) of three holes of diameter  $\varnothing 0.8\text{mm}$  and distance of  $0.2\text{mm}$  between the holes;

case 9 – four groups of three holes  $\varnothing 0.8\text{mm}$  and distance of  $0.2\text{mm}$  between the holes, laying on two mutually perpendicular axes, rotated at an angle of  $45$  degrees in relation to the busbar axes;

case 10 – 2 horizontal groups of 3 holes of diameter  $\varnothing 0.9\text{mm}$  and distance of  $0.1\text{mm}$  between the holes ;

case 11 – two vertical groups of three holes of diameter  $\varnothing 0.9\text{mm}$  and distance of  $0.1\text{mm}$  between the holes;

case 12 - four groups (two horizontal and two vertical) of three holes of diameter  $\varnothing 0.9\text{mm}$  and distance of  $0.1\text{mm}$  between the holes;

case 13 - four groups of three holes  $\varnothing 0.9\text{mm}$  and distance of  $0.1\text{mm}$  between the holes, laying on two mutually perpendicular axes, rotated at an angle of  $45$  degrees in relation to the busbar axes;

Fig. 12 shows the hole shapes of the cases with two groups of small holes (cases 2, 3, 6, 7, 10 and 11).

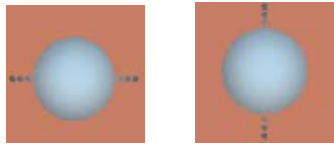


Fig. 12: Hole shape with 2 groups of small holes

Fig. 13 presents the new hole shapes with 4 and 8 groups of small holes (cases 8, 9, 12, 13 and 5).

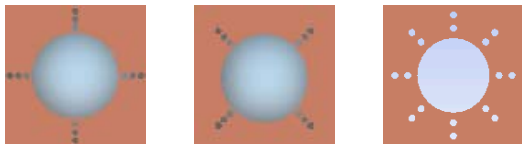


Fig. 13: Hole shape with 4 and 8 groups of small holes

Contact penetration for case 12 is shown in Fig. 14. When the 4 groups of small holes are introduced the high penetration zone expands covering the region between the perforations.

Contact pressure data for the thirteen cases are summarized in Fig.15.

The contact penetration data are generalized in Fig. 16. The aspect of model meshing is distinguished as a key phase for proper analysis of the problem. This is because on the one hand it is an established certainty that the reason for the good quality of physical space triangulation is closely related to the consistent mapping between parametric and physical space.

On the other hand a properly meshed model will present a fairly close-to-reality detailed picture of stress distributions which is a hard task for analytical solution and is usually an averaged value. It is evident from Fig.5, Fig.9 and Fig.14, for the uneven allocation of pressure and penetration, that the 3 investigated designs bring even more complexities.

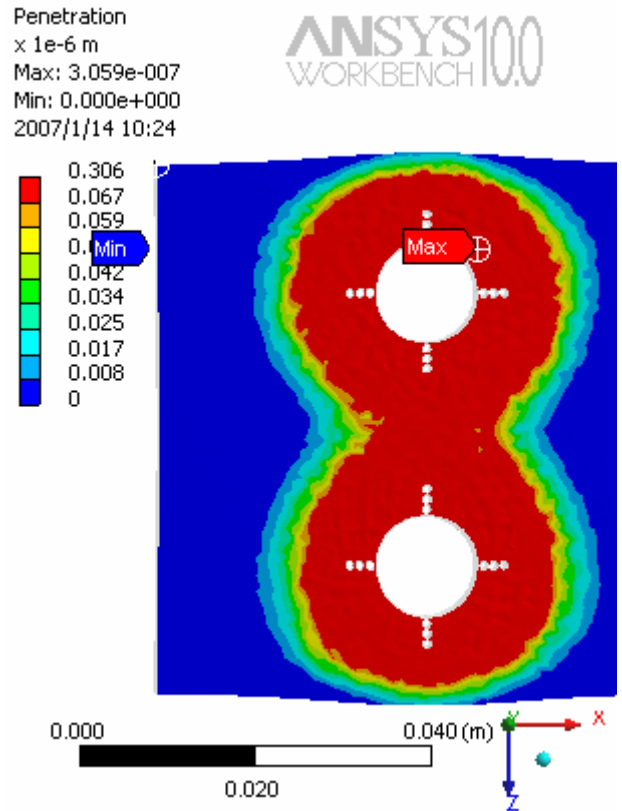


Fig. 14: Case 12 contact penetration

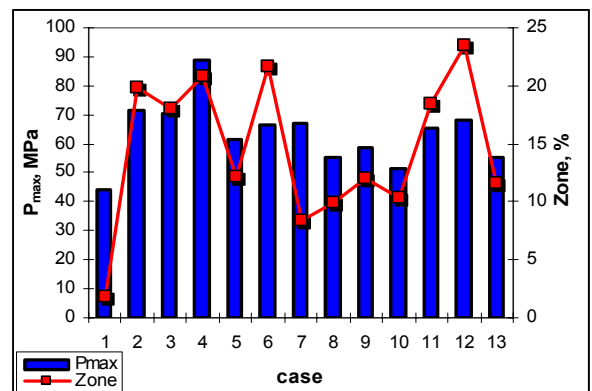


Fig. 15: Max contact pressure and % occupation of the zone of  $P > 38.86\text{MPa}$  for all cases – design G

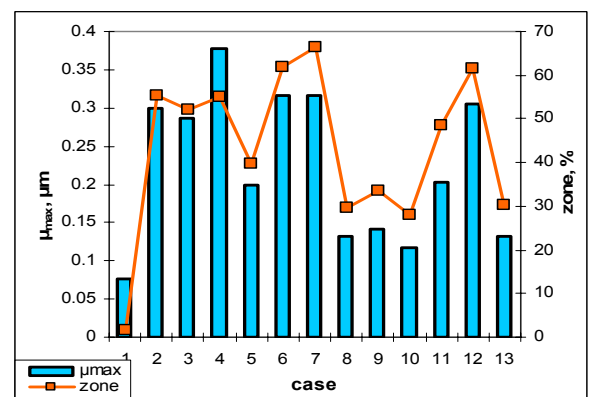


Fig. 16: Max contact penetration and % occupation of the zone of  $\mu > 0.0673\mu\text{m}$  for all cases – design G

In the solving process the meshed models incorporate the following elements: 10-Node Quadratic Tetrahedron, 20-Node Quadratic Hexahedron and 20-Node Quadratic Wedge. Contacts are meshed with Quadratic Quadrilateral (or Triangular) Contact and Target elements.

#### 4. Discussion and conclusions

The models investigated are an abundant source of information for discussions. Here, at this point, for the purposes of conciseness and better outlining, only some of the design cases are stated.

##### Design S

Case 4 has the highest contact pressure of 143.3MPa and the highest penetration value of 0.256 $\mu$ m. The latter occupies 13.84% of the entire model contact area, and is 7 times larger than that for the classic case, Fig. 7

Very good results for contact penetration are obtained for case 11 where the max contact penetration is 0.13 $\mu$ m and the zone of highest penetration is 11 times larger than the corresponding zone in case 1.

##### Design SH

As summarized in Fig.10, cases 2 to 11, show increase in the max contact pressure in the range 12.05÷111.7% higher than the max pressure for the classic case.

The max contact penetration, for cases 2 to 11 is in the range 0.115÷0.327 $\mu$ m i.e. 51.3÷330.3% higher than for the classic case.

##### Design G

In case 4 the max. pressure is 88.73MPa. i.e. 2 times larger than case 1. Additionally the zone of pressure > 38.86MPa occupies 20.83% of the entire contact area while in the classical case it is 1.75% (12 times larger).

The contact penetration for this case is 0.377 $\mu$ m. This value is approximately 5 times the penetration of the classical case 1 (Fig. 16)

The other outstanding case is 12 with max. contact pressure of 67.92MPa and % occupation of the zone of pressure > 38.86MPa – 23.43% ( 13.4 times larger than that for the classical case 1).

Case 12 has max contact penetration 0.306 $\mu$ m and % occupation of the zone of penetration > 0.0673 $\mu$ m – 61.44% (36.35 times the value for the classical case 1).

On the basis of the carried out multitude of investigations, the following could be concluded:

- All the new connection design cases exhibit a significant increase in the contact pressure and penetration. The true area of metal to metal contact is maximized within the electrical interface.
- Despite the difficulties for manufacture, the SH design reveals a smoothly varying contact area behavior for all the cases while the other two designs, S and G, prove to be quite peaked with non stable behavior. In this line of thoughts, the SH design

appears to be less sensitive to manufacturing inaccuracies than the other two designs.

- Single design G cases offer the finest contact pressure and penetration but the average value for all design G cases is around that of the S design or a little below the SH design. Although there seem to be cases in the G design with the zone  $\mu > 0.0673\mu$ m occupying above 60%, the SH design appears to have this same zone with 50% value but on the average.
- Depending on the manufacturing cost, the SH design is a hard-to-manufacture one, but at the same time offers quite a satisfactory contact zone behavior. That is why a compromise between cost and behavior could turn this design out into the most preferable one of all the mentioned designs in this study.

##### *References:*

- [1] R. S. Timsit, "The Technology of High Power Connections: A Review", *20-th International Conference on Electrical Contacts*, Zurich, Switzerland, p. 526, 2002.
- [2] R. Holm, *Electric Contacts, Theory and Application*, Berlin, Germany, Springer-Verlag, 1976.
- [3] V. I. Boychenko, N. N. Dzektsler, *Busbar Connections* (in Russian), Energia, 1978.
- [4] M. Braunovic, Effect of Connection Design on the Contact Resistance of High Power Overlapping Bolted Joints, *IEEE Transactions on Components, Packaging and Manufacturing Technology*, vol. 25, Issue 4, pp. 642-650, Dec. 2002.
- [5] M. Braunovich, Effect of Connection Design on the Performance of Service Entrance Power Connectors, *IEEE Transactions on Components, Packaging and Manufacturing Technology*, vol. 27, Issue 1, pp.72-78, March 2004.
- [6] R. Tzeneva, P. Dineff and Y. Slavtchev, Bolted Busbar connections, *XIV-th International Symposium on Electrical Apparatus and Technologies SIELA'2005*, 2-4 June 2005, Proceedings of papers, vol. I, pp. 207-211, Plovdiv, Bulgaria, 2005.
- [7] R. Tzeneva, Y. Slavtchev, N. Mastorakis and V. Mladenov, Bolted Busbar connections with Slotted Bolt Holes, *WSEAS Transactions on Circuits and Systems*, Issue 7, vol. 5, pp. 1021-1027, July 2006.
- [8] R. Tzeneva, Y. Slavtchev and V. Mladenov, Bolted Busbar Connections with Slotted Bolt Holes, *Proceedings of the 10-th WSEAS Conference on Circuits*, Vouligmani Beach, Athens, pp. 91-95, Greece, July 2006.
- [9] R. Tzeneva, P. Dineff, Bolted Busbar Connections with Particularly Slotted Bolt Holes, *Proceedings of the XLI International Conference on Information, Communication and Energy Systems and Technologies ICES'06*, pp. 371-374, 29-th June-01-st July, Sofia, Bulgaria, 2006.